The EMBO Journal Vol. 22 No. 7 pp. 1707–1715, 2003

Structural organization of authentic, mature HIV-1 virions and cores

John A.G.Briggs, Thomas Wilk, Reinhold Welker[1,2], Hans-Georg Kräusslich[1] and Stephen D.Fuller[3]

The Wellcome Trust Centre for Human Genetics, Division of Structural Biology, University of Oxford, Roosevelt Drive, Headington, Oxford OX3 7BN, UK and [1]Abteilung Virologie, Universitätsklinikum Heidelberg, Heidelberg, Germany

[2]Present address: Abteilung Virologie, Bayer AG, Wuppertal, Germany

[3]Corresponding author
e-mail: stephen.fuller@strubi.ox.ac.uk

J.A.G.Briggs and T.Wilk contributed equally to this work

Mature, infectious HIV-1 particles contain a characteristic cone-shaped core that encases the viral RNA and replication proteins. The architectures of mature virions and isolated cores were studied using cryo-electron microscopy. The average size (~145 nm) of the virion was unchanged during maturation. Most virions contained a single core but roughly one-third contained two or more cores. Consideration of the capsid protein concentration during core assembly indicated that core formation *in vivo* is template-mediated rather than concentration-driven. Although most cores were conical, 7% were tubular. These displayed a stacked-disc arrangement with 7-, 8-, 9- or 10-fold axial symmetry. Layer line filtration of these images showed that the capsid subunit arrangement is consistent with a 9.6 nm hexamer resembling that previously seen in the helical tubes assembled from purified capsid protein. A common reflection (1/3.2 nm) shared between the tubular and conical cores suggested they share a similar organization. The extraordinary flexibility observed in the assembly of the mature core appears to be well suited to accommodating variation and hence there may be no single structure for the infectious virion.

Keywords: capsid protein/cryo-electron microscopy/fullerenes/macromolecular assembly/retrovirus

Introduction

Formation of mature, infectious HIV-1 proceeds through two steps: budding of the immature, non-infectious particle and maturation to the infectious virion (for reviews, see Vogt, 1997; Freed, 1998; Goettlinger, 2001). Particle formation requires the transport of viral Gag polyproteins to the plasma membrane where they associate with other viral and cellular components to produce a budding structure. Virions are released from the cell surface as immature, non-infectious particles containing a spherical layer of Gag polyproteins underneath the viral membrane. The action of the viral protease (PR) on these polyproteins initiates virus maturation concomitant with or after budding (Vogt, 1997). Proteolytic cleavage at defined sites, in a defined order, leads to the formation of the proteins matrix (MA), capsid (CA), nucleocapsid (NC), p6 and two smaller peptides. Proteolytic processing is not required for particle formation or budding. It is required for condensation of the immature, spherical Gag shell to the mature, mostly cone-shaped, core and for the development of HIV-1 infectivity. Prevention of cleavage and maturation using specific inhibitors of the viral PR (Ashorn *et al*., 1990) is a mainstay of current therapeutic regimens for AIDS patients (Sepkowitz, 2001).

Assembly and budding of immature retroviral particles requires only the viral Gag polyproteins (Coffin *et al*., 1997; Vogt, 1997), which assemble at the plasma membrane or in the cytosol, depending on the specific virus. Most likely, assembly is predominantly driven by protein–protein interactions of the C-terminal domains of CA within the Gag polyprotein and is enhanced by membrane association through the N-terminal MA-domain and by RNA–protein interactions mediated by the NC-domain. This leads to three concentric layers of interaction in the Gag shell, yielding a stable protein coat that must be destabilized to prepare for disassembly in the newly infected cell. To achieve this, the Gag shell of the immature particle is dissociated during maturation. Condensation of the inner core structure should therefore be considered as a second assembly step, occurring at millimolar protein concentration in the confined space of the extracellular virion. Protein–protein interactions of CA molecules are likely to promote the formation of the mature CA shell, but the driving force for core formation remains unclear. The process could be driven by the concentration of the CA protein, comparable to the *in vitro* assembly of CA that generates helical tubes. Alternatively, it could be promoted by interaction with the ribonucleoprotein complex (RNP) or another pre-existing structure that would serve as a template for core formation, akin to epitaxial growth (Bergfors, 1999). The template-mediated process would lower the critical concentration for core formation so that the number of cores would reflect the number of templates rather than the CA concentration.

The morphology and architecture of immature and mature HIV-1 particles and other retroviruses has been studied for many years (reviewed in Vogt, 1997). Structural analysis of the immature particle has been facilitated through the expression of Gag polyproteins or domains in tissue culture, to form virus-like particles (VLPs) that share many features with the immature virion. Assembly of spherical particles closely resembling the immature CA shell was even possible in a completely *in vitro* system using bacterially expressed HIV (Gross *et al*., 2000) or Rous sarcoma virus (Campbell and Vogt,

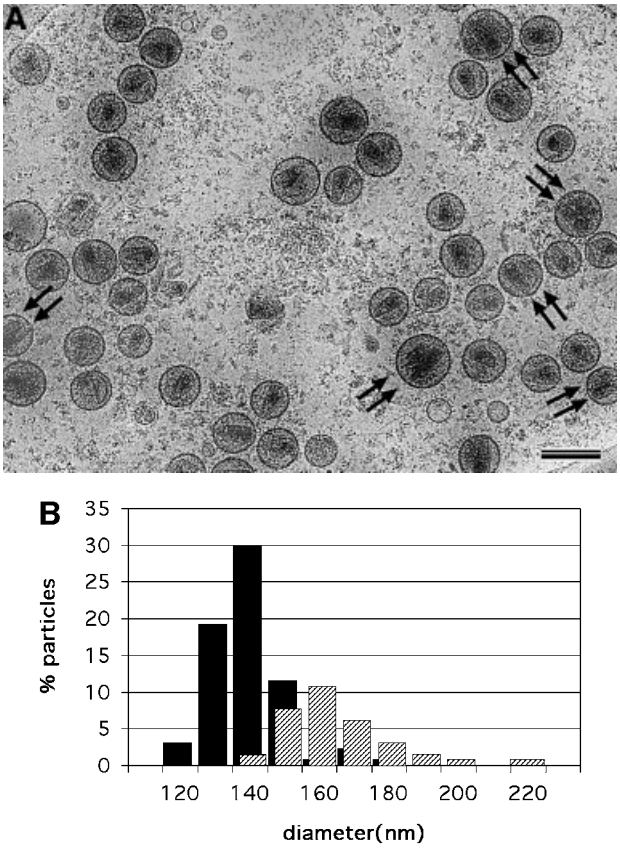

Fig. 1. (**A**) cEM of mature HIV-1. Mature HIV-1 particles were harvested from infected MT-4 cells before a cytopathic effect was established. Virions were inactivated with paraformaldehyde before vitrification. Released virus particles displayed a broad range of diameters, extending from 120 to 200 nm (mean 145 ± 25 nm, $n = 255$). The majority of virions contained a single core, but a significant number of particles (32.6%) contained two or more cores. Virions with a single core were clearly smaller in diameter than virions with two cores (marked with double arrows). Scale bar represents 150 nm. (**B**) The distribution of sizes of HIV-1 virions bearing one and two cores. The distribution of radii is displayed for 132 virions. Particles that appeared to contain more than two cores were excluded. The mean size of the virions containing a single core (134 ± 11 nm, $n = 89$, black bars) was significantly smaller (for equal means, t = 9.3, Prob. = 1.2×10^{-15}) than the mean size of virions containing two cores (158 ± 16 nm, $n = 43$, hashed bars).

1997; Yu *et al*., 2001) Gag-derived proteins. Work on immature particles by negative staining and freeze substitution (Grief *et al*., 1994; Nermut *et al*., 1994, 2002; Kakker *et al*., 1999) suggested that the proteins underlying the surface adopt a hexagonal net. Similar nets have been described in two-dimensional crystals of lipid-linked retrovirus capsid proteins (Barklis *et al*., 1996, 1998; McDermott *et al*., 2000; Mayo *et al*., 2002a,b). Detailed analysis of HIV-1 Gag-VLPs and of authentic immature retroviral particles by cryo-electron microscopy (cEM) revealed that particles are heterogeneous in size and shape and exhibit no overall (e.g. icosahedral) symmetry (Fuller *et al*., 1997; Yeager *et al*., 1998; Wilk *et al*., 2001), but show areas of local symmetry (Fuller *et al*., 1997; Wilk *et al*., 2001). The architecture of the immature virus appears relatively simple: the uncleaved Gag polyproteins are arranged radially with the MA domains at the membrane and the C-terminal ends pointing inward (membrane-MA-CA-NC-p6) (Wilk *et al*., 1999). This radial sequence is maintained in the mature virion. A layer of MA proteins remains beneath the membrane, while the processed CA proteins form the shell of the mature core (Gelderblom *et al*., 1987). The RNP including the viral replication proteins, forms within this core by condensation of the genome with NC.

The biochemical and structural characterization of the morphologically defined mature HIV-1 core has been difficult. Removing the envelope of the mature virion by detergent treatment led to rapid disintegration of the inner structures. Recently developed protocols have allowed preparation of intact cores for negative-stain EM and biochemical analysis (Kotov *et al*., 1999; Accola *et al*., 2000; Welker *et al*., 2000). These studies provided an overview of the core geometry, documenting its variability and the approximate ratio of its constituents (Welker *et al*., 2000). Studies on *in vitro* assembled particles have shed additional light on core formation. Retroviral CA as well as longer proteins containing the NC domain (e.g. CA-NC) assemble *in vitro* into helical tubes with diameters between 300 and 800 Å and lengths of up to several microns (Ehrlich *et al*., 1992; Campbell and Vogt, 1995, 1997; Gross *et al*., 1997; Ganser *et al*., 1999). Helical reconstruction of HIV-1 CA tubes (Li *et al*., 2000) from several helical families showed that they are formed of hexameric rings of CA protein. The hexamer displayed an exterior diameter of ~100 Å surrounding a central hole of ~25 Å diameter. The radial arrangement of the CA protein was similar to that in the immature virion. The N-terminal CA domain was located on the outside and the observed ~72 Å thickness corresponded to the long axis of the CA subunit in Gag.

Purified HIV-1 CA protein can also assemble to form conical structures that are reminiscent of the authentic HIV core (Ganser *et al*., 1999), suggesting that the *in vitro* assemblies are relevant to the cores found in the virus, but the structure and formation of the core within the authentic virion has not been analyzed to date. Ganser *et al*. (1999) proposed that the core maintained local 6-fold symmetry by forming a fullerene cone. A hexagonal net can be closed by the inclusion of 12 pentagons. These are equally spaced to close the net in an icosahedron (Caspar and Klug, 1962). When the pentagons are arrayed so that six are at either end of an elongated structure, a tube results. An uneven distribution of pentamers, such as five at one end and seven at the other, results in a closed cone-like structure. This is well described by Ganser *et al*. (1999) and the reader is directed to this paper for a complete explanation and related references.

Here, we present a cEM analysis of mature HIV-1 particles obtained from infected T cells and of virion-derived cores. These studies extend the *in vitro* experiments by addressing two issues. The first is the relevance of the helical tubes to the architecture of authentic HIV cores. We show that the basic unit of the authentic, mature core is consistent with a hexamer that appears similar to the one forming the *in vitro* helical tubes. The second is the effect of the conditions of core formation in the virion. These are quite distinct from those used for *in vitro* assembly studies. The frequent observation of multiple cores within single virions, combined with the calculation of the CA protein concentrations during core formation,

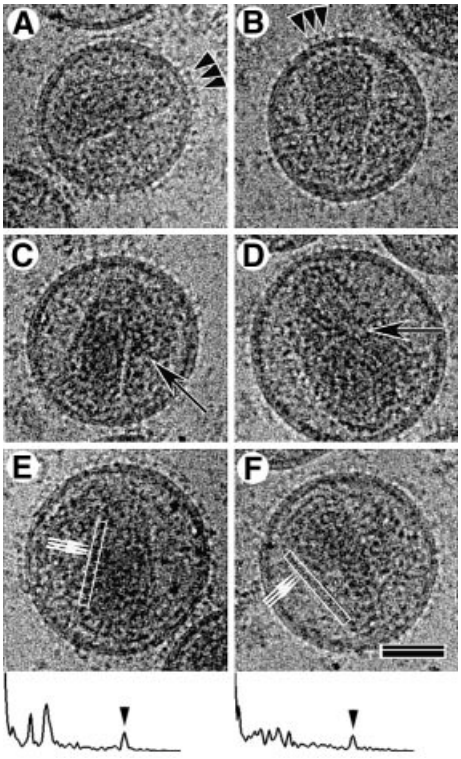

Fig. 2. cEM analysis of the mature virion. Most mature virions displayed regular membrane projections (**A** and **B**, arrowheads) and contained cone-shaped cores. Many particles contained a complete second core, which can be conical, tubular (**C** and **D**, arrows) or amorphous. cEM allowed the visualization of the regular arrangement of core subunits (small arrows in **E** and **F**), which were spaced at 3.2 ± 0.48 nm, $n = 60$. The power spectra of the boxed regions demonstrating the presence of the 3.2 nm repeat (arrowheads) along one side of the cone are shown below panels (E) and (F). The broad end of the conical core was usually located in proximity to the membrane; however, no connection could be observed. The scale bar represents 50 nm.

suggests that the assembly process is template-mediated rather than concentration-driven as it is *in vitro*.

Results

The organization of mature HIV-1

We obtained a concentrated, high-titer (~10^9 infectious units per ml) HIV-1 preparation containing minimal cellular contaminants by combining a high-multiplicity infection with harvesting at early time points and rapid purification of virus (Welker *et al*., 2000). SDS–PAGE analysis of the concentrated preparation showed that the Gag proteins were the main constituents and there was minimal contamination with cellular proteins (data not shown). Virus particles were pelleted through a cushion of sucrose and vitrified immediately as described previously (Fuller *et al*., 1997). Rapid sample preparation minimized deleterious effects on the particle structure. Typical samples showed a large number of mature HIV-1 particles and lacked large, membranous, cellular contaminants (Figure 1A). The diameter of the mature particles (145 ± 25 nm, $n = 255$) was very similar to that previously reported for immature particles (139 ± 16 nm, $n = 197$) (Wilk *et al*., 2001). The interiors of most particles contained a central, dense core structure. Some density was observed within the virion outside the core. No structures that could correspond to the previously reported lateral bodies (Gelderblom *et al*., 1987) were visible. Immature virions were rarely observed and represented <1% of the preparation.

Images of vitrified mature HIV-1 showed closely packed patches of surface projections, extending ~7.5 nm from the virion surface (arrowheads in Figure 2A and B). Analysis of the density distribution within the lipid bilayer (data not shown) indicated that it had the same three-layered appearance as observed for immature HIV-1 (Wilk *et al*., 2001) and the VLPs resulting from Gag expression (Fuller *et al*., 1997). The majority of the enveloped virus particles in the preparation contained a single core structure. Surprisingly, a significant fraction of the mature particles contained a second core assembly (32.6%, $n = 132$) (Figure 1A, double arrows; Figure 2C and D, arrows). Particles containing three distinct cores were observed very rarely. Most cores exhibited a conical shape but a small fraction showed a tubular or amorphous morphology. Mature HIV-1 particles containing two cores had a significantly larger particle diameter (159 ± 16 nm) than particles with only one core (134 ± 11 nm) (Figure 1B). When two or more cores were observed they appeared to be roughly the same size as the cores in virions that contained only one, although overlap of the two cores made it difficult to determine this precisely.

Closer examination of the images revealed that the ends of the conical cores were often located near the viral membrane (Figure 2). A gap was usually observed between the inner leaflet of the membrane and the core. This makes the presence of a solid physical link (Gelderblom, 1991) between the membrane and the viral core unlikely. A regular arrangement (3.2 ± 0.5 nm, $n = 60$) of subunits could often be seen along one edge of assembled cores (Figure 2E and F, arrows and power spectra of boxed regions). Such a repeating feature gives rise to a diffraction peak in the power spectrum of the image (see below).

Morphology of core particles isolated from mature HIV-1

HIV-1 preparations produced as described above were lysed with detergent to isolate cores. After treatment with 0.5% Triton X-100 for 2 min, cores were collected by a brief spin in a microcentrifuge as described previously (Welker *et al*., 2000). Analysis of the core preparation by cEM revealed a large number of intact cores lacking the viral membrane (Figure 3). Isolated cores were heterogeneous in size and shape with a morphology similar to that observed in complete virions. The preparation contained predominantly cone-shaped core structures of various sizes, as well as a minor fraction of tubular (Figure 3, arrows) and polymorphic shapes. Many cores exhibited a region of increased density at the broad end of the cone (Figure 3, arrowheads), which is likely to correspond to the viral RNP.

Measurements of the overall length, diameter and the cone angle at the narrow end were performed for 267 conical cores. Cores were excluded if they appeared to be damaged or acutely tilted so that all three parameters could not be measured reliably. As shown in Figure 4, the three parameters showed nearly Gaussian distributions with a

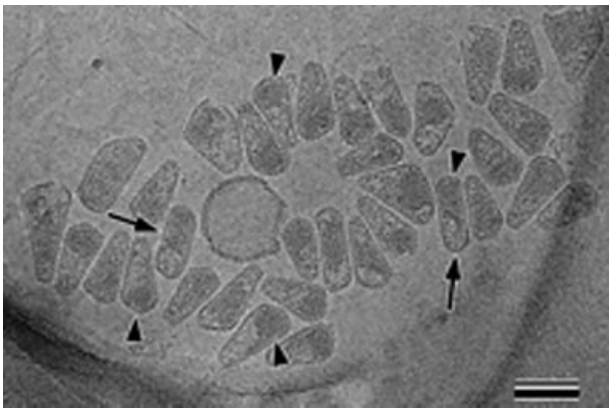

Fig. 3. Overview of isolated HIV-1 cores in cEM. Intact cores were prepared by brief detergent treatment and centrifugation in a microcentrifuge as described (Welker *et al.*, 2000). This figure shows a representative cEM image depicting isolated cores of heterogeneous size and shape. The majority of the isolated cores displayed a conical shape while a minor fraction was found to be tubular (~7%, arrows). In most cases, the regular arrangement of the wall subunits was preserved. Many cores showed an increased density at the broad end, presumably due to the condensed viral RNP in this position (arrowheads). The scale bar represents 100 nm.

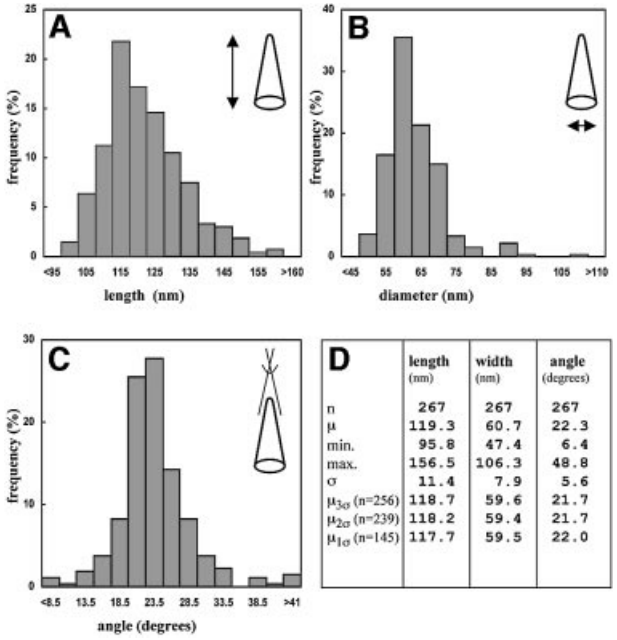

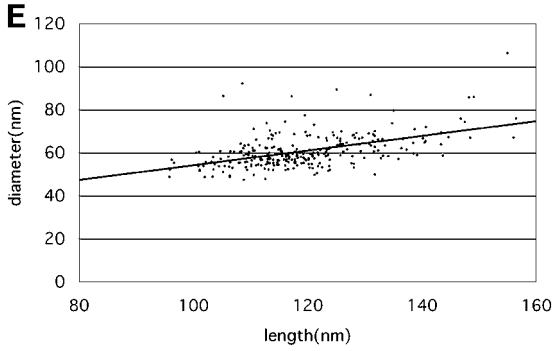

Fig. 4. Size and geometric variation of HIV-1 cores. The histograms show the distribution of length (**A**), diameter (**B**) and angle at the narrow end (**C**) of conical HIV-1 cores. Length and diameter were measured once for each core, while the mean of three independent measurements was used in case of the angle. Particles were excluded if the standard deviation of three measurements for the cone angle was >15% of the respective mean, or if all three parameters could not be measured. Arbitrary size classes were defined for each parameter, and the frequency of cores found for each class was plotted. (**D**) A tabulated version of the results. Abbreviations: *n*, number; μ, mean; min., minimal value; max., maximal value; σ, standard deviation; $\mu_{3\sigma}$, $\mu_{2\sigma}$ or $\mu_{1\sigma}$, mean calculated from the fraction of particles within the range of three (n = 256), two (n = 239) or one (n = 145) standard deviation of the overall mean, respectively. The correlation between the width at the broad end of the core and the overall length is shown in (**E**). The slope of the line corresponded to an included angle of 19.7 ± 2°.

slight positive skew. The average particle length (119 ± 11 nm) was measured along the central core axis and the maximum diameter (60 ± 8 nm) was measured perpendicular to this axis (Figure 4A, B and D). Measurement of the angle at the tip of the core gave 22 ± 6° (Figure 4B), and was associated with a larger degree of variation than measurements of length and diameter (Figure 4D). The potential impact of a few aberrant cores was evaluated by recalculating the means using only the particles within the 3σ, 2σ or 1σ ranges. The resultant means ($\mu_{3\sigma}$, $\mu_{2\sigma}$ and $\mu_{1\sigma}$ in Figure 4D) varied only marginally (<2.7%) from those calculated for the whole data set. Hence the variance in the values represents the true variation in the population rather than the contribution of a few outliers.

We reasoned that the effect of tilt on apparent cone angle should appear in a comparison of long cores (which must lie relatively parallel to the water layer) with short ones (which can adopt a more acute angle within the layer). Plotting the width of the broad end of the core versus its length (Figure 4E) yielded a correlation coefficient of 0.35 ± 0.04, corresponding to an included angle of 19.7 ± 2.1° [$2\tan^{-1}(0.35/2.0)$]. This provided further evidence for the overall conical shape of the core. We observed no correlation between this derived cone angle and length (Figure 4E). Hence, tilt did not significantly affect the apparent cone angle to within the precision of these measurements. Any possible effect of tilt on the measurements would be small; a consistent 10° tilt in the cores would only increase the apparent cone angle by ~1°.

The structural organization of authentic, mature HIV-1 cores

The removal of the viral membrane allowed us to examine the ends of the isolated cores closely. Cores appeared to be closed structures. Examination of individual cores in single (Figure 5) and stereo images (data not shown) revealed continuous density along the ends rather than the broken density that would indicate a hole. The appearance of conical cores was complex because of the superposition of the two sides of the structure seen in the cEM image. The 3.2 nm spacing between repeating units was most easily seen along the long edges of the core (Figure 5C, boxed region, and D), as it was in the intact virions. Repeating units were never clearly seen on both edges of the same core as expected for a fullerene cone (see below and Li *et al.*, 2000).

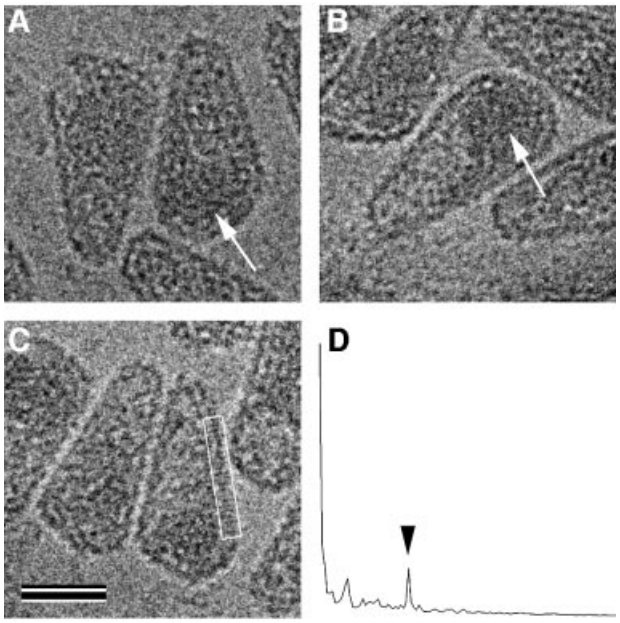

Fig. 5. Isolated HIV-1 cores retain well-ordered subunits and terminal structures on both ends. (**A**–**C**) Typical cores appeared closed at both ends. The white arrows mark the positions of density that we presume to correspond to the RNP in the cores. The scale bar represents 50 nm. The power spectrum of the region boxed in (C) is shown in (**D**). The detergent treatment had little effect on the regular arrangement of CA subunits, as indicated by the preservation of the ~3.2 nm reflection (arrowhead).

The packing of subunits in the conical cores was difficult to analyze. The classical tools of Fourier analysis that are appropriate for crystalline or helical structures exploit the fact that the substructure repeats with a defined distance and hence gives rise to diffraction maxima in a power spectrum. An arrangement of subunits that generates a conical structure does not repeat with distance. The power spectrum of such an object will not display, for example, the sharp layer lines of a helical object. The cores that displayed a tubular morphology (~7% of the total, 18 of 267) were more tractable (Figure 6A) since they did display a simple repeating pattern as evidenced by the lines comprising the power spectra (Figure 6B). We therefore focused on these tubular cores for analysis.

Nineteen of 25 apparently tubular cores analyzed exhibited peaks in their power spectra. Eighteen of these cores showed similar power spectra and were analyzed further. Tubular cores had an average diameter of 44.3 ± 4.3 nm. Their lengths (119.7 ± 20.1 nm) were similar to the length of conical cores. Figure 6B shows the computed power spectrum of a tubular core (raw image in Figure 6A) that displayed peaks corresponding to the repeated distances in the structure. These layer lines were simple multiples of ~9.6 nm (9.6 ± 0.3 nm). Distinct classes of tubular cores could be distinguished by their diameters. The observed diameters were multiples of 5.4 ± 0.2 nm (N = 7, 8, 9, or 10 with R = 0.96). The positions of the diffraction maxima (Figure 6C; Supplementary data available at *The EMBO Journal* Online) did not vary with core diameter as shown in Figure 6G, in which tube diameter was plotted against the repeat distances for the tubular cores analyzed in this study. This differs from the case with classical helical symmetry, such as the *in vitro*-assembled CA tubes (Li *et al*., 2000), in which the spacing of the layer lines varies with the tube diameter.

Image processing revealed the structure of the repeating unit. Correcting the contrast transfer function (Erickson and Klug, 1971; Mancini and Fuller, 2000; Mancini *et al*., 2000) on the individual images and summing the aligned defocus pairs prior to filtering enhanced the contrast. These operations increased the strength of the layer lines but did not affect the symmetry of the resulting image. The fact that information about the repeating unit is found on the layer lines allows one to filter the transform and back transform to show the repeating unit. Selecting the strongest layer lines (which are multiples of 1/9.6 nm) (Figure 6E) and zeroing the transform between them generated a filtered image of the repeating unit (Figure 6D). A 2-fold symmetry is evident in Figure 6D (2-fold phase residual 34°, where a residual of 0° would correspond to perfect 2-fold symmetry and 90° to random). Application of this 2-fold symmetry to the filtered image yielded the projection shown in Figure 6F for this N = 8 tubular core. The filtered, averaged image showed a hexameric unit with a diameter of ~9.6 nm. The clarity of the hexamers in Figure 6 reflects the fortuitous occurrence of a tube that is almost directly perpendicular to the direction of view and in the proper axial rotation. In this tube, the hexamers on the top and bottom superimposed. A small tilt would have generated a projection in which the hexamers in the body of the tube interfere and produced a less interpretable image. Our conclusion that hexamers comprise the tubes rests on the conservation of the repeat distance and the quantized distribution of diameters that matched that expected for a hexagonal array. Figure 7 is an illustration of this arrangement that is consistent with the statistical analysis of the tube geometry.

Discussion

A detailed understanding of the formation of infectious HIV-1 particles requires structural information regarding the mature virion, its assembly intermediates and the relevant building blocks. Our current knowledge regarding the structure and organization of authentic mature HIV-1 virions and cores is mainly derived from conventional EM. Here, we report a cEM study of mature, infectious HIV-1 particles that extends our previous work on immature virions (Wilk *et al*., 2001) in order to characterize the authentic virion. These studies document the intrinsic variability of HIV-1 particle sizes and shapes and suggest the consequent robustness of the assembly process. HIV-1 assembly does not follow an exact blueprint for the production of identical particles but rather obeys rules that result in the production of variable particles.

The intact mature virion

Intact mature HIV-1 particles displayed projecting spikes on the surface, which are likely to correspond to the viral glycoproteins. Our previous analysis of immature HIV-1 particles revealed a comparable density of surface projections (Wilk *et al*., 2001). The lipid bilayer itself displayed the same overall organization as reported for immature HIV-1. The dense layer of protein located just below the

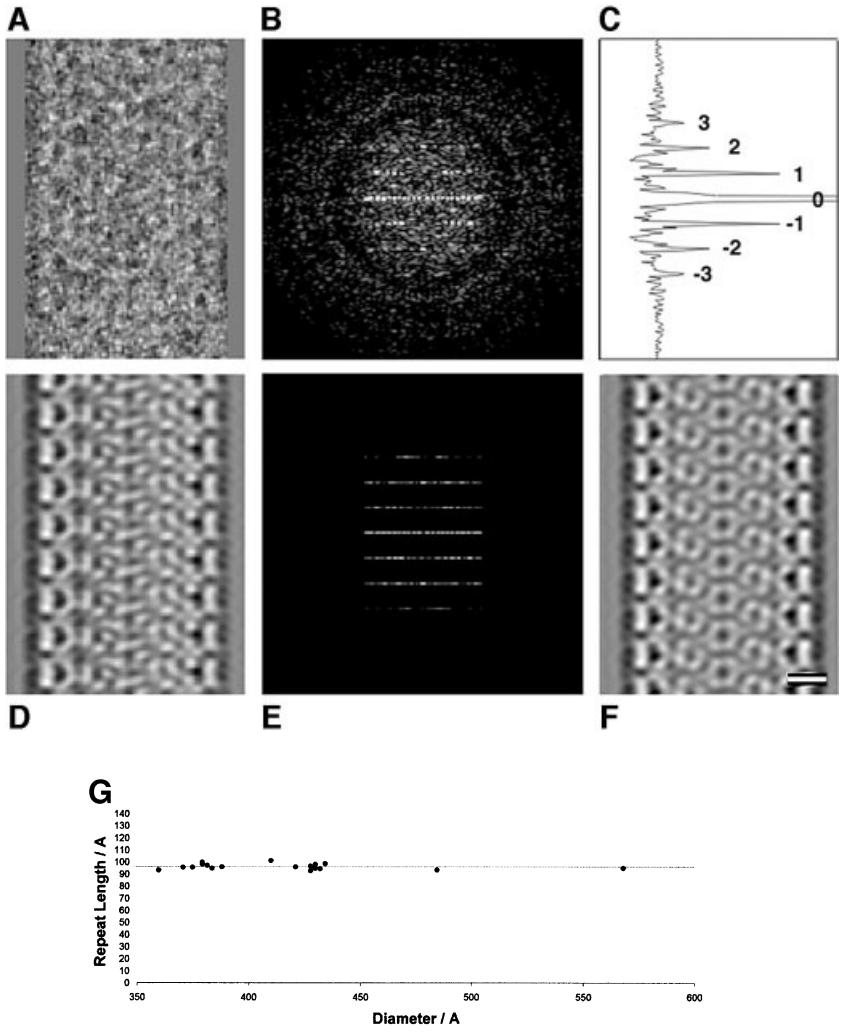

Fig. 6. Image processing of a tubular core. The steps of image processing are shown for a tubular core. (**A**) The raw image of the isolated core. The power spectrum of this core is shown in (**B**), with the corresponding collapsed intensity profile in (**C**). The orders of the 1/9.6 nm reflections were labeled. Suppression of the off-layer line noise in (B) gives the filtered power spectrum in (**E**). The corresponding layer line filtered image is shown in (**D**). (**F**) The image in (D) after application of 2-fold symmetry. (**G**) The repeat length of the tubular cores is independent of their diameter. The scale bar in (F) represents 10.0 nm.

membrane and attributed to the MA domain of Gag in the immature particle (Fuller *et al*., 1997; Wilk *et al*., 2001) was maintained in the mature particle. Comparison of the average sizes of authentic mature and immature HIV-1 particles revealed that maturation occurs without a significant change in diameter.

Architecture of isolated cores

cEM analysis confirmed that the variation in size and shape previously observed for negatively stained cores (Welker *et al*., 2000) was an intrinsic property of the core rather than a reflection of dehydration or preparation for EM. Similar results were recently reported for Rous sarcoma virus (Kingston *et al*., 2001; Yu *et al*., 2001). cEM yielded larger values for the length (119.3 nm) and width (60.7 nm) of isolated cores in comparison with the values measured by negative staining (102.9 and 52.4 nm, respectively (Welker *et al*., 2000). This presumably reflects the lack of shrinkage in the hydrated samples. *In vitro*-assembled cores varied in length between 100 and 300 nm (Ganser *et al*., 1999). Comparison of the cEM images of cores within mature virus with those of the isolated cores revealed that both display the characteristic 3.2 nm edge repeat, indicating that the isolation procedure did not significantly distort the core.

Ganser *et al*. (1999) presented an elegant fullerene cone model for the HIV core based on the structure that their group determined for *in vitro*-assembled helical tubes of CA protein (Li *et al*., 2000). The fullerene model predicts that core assemblies will adopt one of a set of defined geometries. These geometries permit the preservation of hexagonal (p6) symmetry in the lattice with 12 pentameric vertices allowing the curvature of the structure to produce a closed core. Ganser *et al*. (1999) showed that CA-NC assembles *in vitro* with RNA to adopt a set of included cone angles (19.2, 38.9, 60, 83.6 and 112.9°) corresponding to the defined set of fullerene cone geometries (Ge and Sattler, 1994). The 19.2° species (corresponding to five

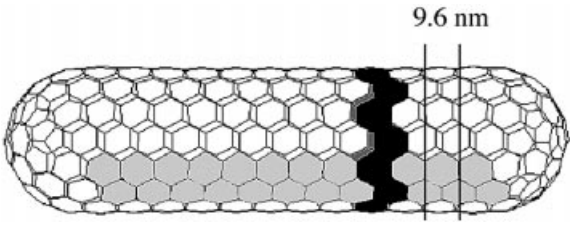

Fig. 7. Schematic of a stacked-disc fullerene tube. The figure illustrates one possible structure of a stacked-disc fullerene tube. One disc in the stack is shaded black. Removing or adding a strip of hexamers such as that shaded in gray varies the width of the tube body. The tube shown is formed from eight such strips. The tube ends illustrated represent one of a number of possible constructions. The 9.6 nm repeat is marked.

pentamers at the narrow end and seven at the wide end) formed the majority of the population. The authors suggested that authentic HIV-1 cores should follow the same distribution of angles. Our Fourier filtered images of tubular cores (Figure 6) revealed a hexagonal unit in authentic HIV-1 cores. The size of this hexamer was similar to that seen by Li *et al*. (2000), providing direct evidence that the hexameric unit seen in *in vitro*-assembled CA tubes is indeed relevant to the authentic core. The fact that the tubular cores shared the 3.2 nm spacing with the conical ones suggests that the local packing of the hexamers was similar in both structures. The observed variation in the size and end shape of the conical cores can be accomodated in the fullerene cone model by variation of the number of hexamers and the precise positioning of the pentameric defects. The average angle of the authentic cores (22 ± 5°) was very similar to the 19.2° predicted by fullerene cone geometry. The authentic conical cores appeared to be more restricted in their included angle than the *in vitro*-assembled ones, since only the 19.2° cones were observed. This may reflect biological control of core assembly.

The filtered, symmetrized image of a tubular core (Figure 6F) could be interpreted as layers of hexamers. The hexamers in alternate layers were staggered relative to each other so that the layers were paired. The paired layers formed discs that repeated with a constant spacing of 9.6 nm. This arrangement of hexameric units is illustrated in Figure 7. It corresponds to a degenerate case of helical symmetry called a 'stacked disc'. Such an arrangement has been observed previously in several biological contexts, most notably as an intermediate in tobacco mosaic virus assembly (Butler and Klug, 1971). The particular arrangement of stacked discs has also been described for fullerene tubes, where it is denoted the 'armchair' form because the hexamer edges are perpendicular to the long axis of the tube (Yacobsen and Smalley, 1997).

The observed 9.6 nm reflection is caused by the spacing of the hexamers (marked in Figure 7). The discrete variation in tube diameter would correspond to the removal or addition of pairs of strips of hexamers (7, 8, 9 or 10) (Figure 7) along the length of the tube. This would alter the circumference by multiples of 16.6 nm and change the diameter by multiples of 5.3 nm, which is indistinguishable from the observed 5.4 ± 0.2 nm. The 3.2 nm reflection must result from features within the hexamer such as domains of the individual proteins coinciding with the third order of the 9.6 nm repeat. The packing in the tubular cores provides some insight into the arrangement in the conical ones. The edges of the conical cores showed a reflection of 3.2 nm (3.2 ± 0.5 nm, $n = 60$). The tubular cores also showed a 3.2 nm reflection. Hence, local packing of the hexamers was similar in the two structures although the overall arrangement that results in the formation of the tubular core must differ from the one that results in a conical core. A more complete determination of the structure of the conical cores will require the use of methods, such as tomography, that do not require averaging of this variable structure.

Formation of multiple cores: implications for the mode of assembly

The presence of HIV-1 particles with multiple cores has been noted previously (e.g. Gelderblom, 1991); however, they were seen as rare events. Previous analyses of HIV-1 particles used primarily thin-section electron microscopy, which will only detect multiple cores if they both lie within the plane of the section and present a recognizable profile. Indeed, the fact that multiple cores have been observed by conventional methods at all suggests that they are not rare events. Our cEM analysis of mature HIV-1 preparations showed that roughly one third (32.6%) of the mature particles contained two discrete core structures. Multiple cores were also common in other preparations of HIV-1 and of HIV-2 (J.A.G.Briggs, J.Daeke, H.-G. Kräusslich and S.D.Fuller, manuscript in preparation).

Virions containing two cores were larger on average than those containing a single core. This observation has implications for the mechanism of core formation. Two fundamentally different mechanisms can be distinguished. Core formation could be driven by the concentration of CA protein, as it is during assembly of helical tubes *in vitro*. Multiple cores would form when the CA concentration exceeds the threshold required for assembly. Alternatively, a template, such as the RNP, could initiate core formation. Multiple cores would form in a virion when it contained multiple templates. Our measurements of the virion diameters led to a quantitative picture of core formation that distinguishes these possibilities.

Recent scanning transmission EM measurements of the similarly sized Mason–Pfizer monkey virus (1900–2100 molecules; Parker *et al*., 2001), allows one to estimate that the average HIV-1 particle contains ~2100 Gag monomers. These values would correspond to a CA concentration of 3.5 mM (1.8 mM dimers since Gag and CA are believed to be dimeric; Gamble *et al*., 1997; Scarlata *et al*., 1998; Worthylake *et al*., 1999). Provided that the Gag–Gag spacing in small and large particles is the same, one can predict that the group of larger particles (159 nm diameter; Figure 1B) that contained two cores will have a lower CA concentration (1.5 mM dimers) than the group of smaller (134 nm) particles with a single core (1.8 mM) because the ratio of surface area to volume decreases with radius.

The number of CA molecules consumed by the formation of a cone can be estimated from the packing density in the helical assemblies (Li *et al*., 2000) and from the measurements of cone angle, length and maximum width, giving 625 dimers when the effect of the end

structures is considered. The tubular cores described here should contain ~550 dimers. Formation of the first core therefore leaves concentrations of 0.70 and 0.72 mM CA dimers in the small and large particles, respectively, which is not sufficiently different to explain formation of a second core only in the latter case. At no point before or after formation of a single core is the CA concentration in the larger double-cored particles higher than that in the smaller single-cored particles and hence concentration cannot drive initiation of formation of multiple cores. Taken together, these considerations suggest that core formation during HIV-1 maturation is template-mediated. This conclusion is strengthened by recent scanning transmission EM measurements, which suggest that our current estimate of the total amount of CA protein in a virion may be too low (J.A.G.Briggs, M.C.Johnson, M.Simon, I.G.Gross, H.-G.Kräusslich, V.M.Vogt and S.D.Fuller, manuscript in preparation).

Why would larger particles be more likely to contain multiple templates? Possible templates include the RNP-complex, factors at the site of membrane closure upon virion release, and protein complexes formed upon initiation of polyprotein processing (e.g. CA pentamers). However, the latter two would not explain easily why particles containing two templates are larger on average. The domain model for immature particle formation (Fuller *et al*., 1997) suggests that larger particles would be formed by the accretion of smaller, RNA-containing domains. Immature particles consisting of two half-shells of Gag as well as confluent viral buds have been observed by thin-section EM analysis (Gelderblom *et al*., 1987, Gelderblom, 1991; Vogt, 1997). Incorporation of multiple RNAs could lead to formation of separate RNPs and hence separate templates. The hypothesis of RNP-template nucleated CA condensation would be consistent with the organization of assembly domains and the order of cleavages. The C-terminal region of CA, the adjacent spacer peptide and NC appear to form a continuous assembly domain, essential for formation of the immature virion, and also for packaging the RNA genome. Release of the RNA-associated NC is a first step in Gag polyprotein cleavage, which destroys this assembly domain, separates CA from NC and allows condensation of the RNP that could subsequently function as a template for CA condensation. If multiple cores are indeed due to the presence of multiple RNP templates, one would predict that a significant number of virions contain four copies of RNA (two RNA dimers). If infectious, such tetraploid virions could increase the potential for recombination.

Materials and methods

Cell culture and virus preparation

High-titer virus preparations were produced as described previously (Welker *et al*., 2000). Briefly, MT-4 cells were maintained at 37°C, 5% CO_2 in RPMI-1640 supplemented with 10% heat-inactivated fetal calf serum, 100 U/ml penicillin, 100 μg/ml streptomycin, 4 mM glutamine and 5 mM HEPES. Stocks of HIV-1 strain NL4-3 (Adachi *et al*., 1986) were produced by transfection of HeLa cells. MT-4 cells were initially infected with cell-free virus, and infected cultures were subsequently expanded by co-cultivation. Virus preparations for isolation of HIV-1 cores were harvested before pronounced cytopathic effects were observed (24–32 h post-infection). Virus-containing supernatants were cleared by low-speed centrifugation, filtered through 0.45 μm pore-size cellulose-acetate filters (Schleicher and Schuell) and analyzed for antigen content. Infectious titers of virus preparations were at least 2×10^7 $TCID_{50}$ per ml (tissue culture infectious dose 50% per ml) as determined by endpoint titration (Welker *et al*., 2000). Virus particles were concentrated from cleared culture medium by centrifugation through a cushion of 20% (w/w) sucrose in phosphate-buffered saline (PBS) at 130 000 *g* for 2 h at 4°C. The pellet was slowly resuspended in PBS (~3.5 μl/ml initial culture volume). Prior to vitrification, intact HIV-1 particles were inactivated with 2% paraformaldehyde in buffer for 30 min on ice.

Isolation of HIV-1 cores

For isolation of virus cores (Welker *et al*., 2000), 40 μl of fresh virus suspension were mixed with an equal volume of 200 mM NaCl, 100 mM MOPS pH 7.0, and virions were lysed for 2 min at room temperature by adding Triton X-100 to a final concentration of 0.5%. HIV-1 cores were recovered by centrifugation in a microcentrifuge at full speed (13 800 *g*) for 8 min at 4°C. The pellets were washed twice with 100 mM NaCl, 50 mM MOPS pH 7.0, and resuspended in 8 μl of the same buffer. Core suspensions were processed immediately for further analysis without fixation.

Microscopy and image analysis

cEM was performed as described previously using a Philips CM200FEG operated at 200 kV at a magnification of 38 000× (Fuller *et al*., 1997; Wilk *et al*., 2001). Micrographs were digitized on a Zeiss SCAI scanner (Oberkochen, Germany) at a step size of 14 μm or a UMAX 3000 scanner at 8 μm step size. This is equivalent to 2.19 Å/pixel for the images analyzed for the reconstruction in Figure 6. Measurements were performed using the SPIDER image analysis program (Frank *et al*., 1996). The particle size was measured from the outer leaflet of the membrane and thus excludes the contribution of the viral glycoproteins. The defocus was determined from the positions of the local minima in a radially averaged power spectrum of the micrographs. We divided the transform of the image with the appropriate phase contrast transfer function (CTF) to correct its effect as described previously (de Haas *et al*., 1999; Mancini and Fuller, 2000; Mancini *et al*., 2000). Images were aligned by cross correlation after CTF correction and then layer line filtered and 2-fold averaged to produce the final projection. The 2-fold phase residual was calculated by cross-correlating the 2-fold rotated image with the original.

Measurements of length, diameter and angle of isolated cores were performed as described previously (Welker *et al*., 2000) using the SigmaScan software package (Jandel Scientific). Statistical analysis was performed using Microsoft Excel.

Supplementary data

Supplementary data are available at *The EMBO Journal* Online.

Acknowledgements

We thank Professor David Manolopoulos (Physical and Theoretical Chemistry Laboratory, University of Oxford) for a useful discussion of nanotubes and their energetics and providing the PDB file upon which Figure 7 is based. We are also pleased to acknowledge our colleagues Brent Gowen, Dr Rishi Matadeen and Professor David Stuart (WTCHG, University of Oxford) for helpful discussions and Dr Barbara Muller (Abteilung Virologie, Universitätsklinikum Heidelberg) for careful reading of the manuscript. We are also grateful to Professor Wesley Sundquist (University of Utah) for discussions and the sharing of results prior to publication. We acknowledge the support of the Deutsche Forschungsgemeinschaft (FU 386/1; KR 906/2) and the Wellcome Trust (HH5FE) for this work. J.A.G.B. holds a Wellcome Trust Structural Biology Studentship. S.D.F. is a Wellcome Trust Principal Research Fellow.

References

Accola,M.A., Ohagen,A. and Gottlinger,H.G. (2000) Isolation of human immunodeficiency virus type 1 cores: retention of Vpr in the absence of p6(gag). *J. Virol.*, **74**, 6198–6202.

Adachi,A., Gendelman,H.E., Koenig,S., Folks,T., Willey,R., Rabson,A. and Martin,M.A. (1986) Production of acquired immunodeficiency syndrome-associated retrovirus in human and nonhuman cells transfected with an infectious molecular clone. *J. Virol.*, **59**, 284–291.

Ashorn,B., McQuade,J.M., Thaisvivongs,S., Tomasselli,A.G., Tarpley, W.G. and Moss,B. (1990) An inhibitor of the protease blocks

maturation of human and simian immunodeficiency virus and the spread of infection. *Proc. Natl Acad. Sci. USA*, **87**, 7472–7476.

Barklis,E. *et al.* (1996) Structural analysis of membrane bound retrovirus capsid proteins. *EMBO J.*, **16**, 1199–1213.

Barklis,E., McDermott,J., Wilkens,S., Fuller,S. and Thompson,D. (1998) Organization of HIV-1 capsid proteins on a lipid monolayer. *J. Biol. Chem.*, **273**, 7177–7180.

Bergfors,T.M. (ed.) (1999) *Protein Crystallization: Techniques, Strategies and Tips*. International University Line, La Jolla, CA.

Butler,P.J. and Klug,A. (1971) Assembly of the particle of tobacco mosaic virus from RNA and disks of protein. *Nat. New Biol.*, **229**, 47–50.

Campbell,S. and Vogt,V.M. (1995) Self-assembly *in vitro* of purified CA-NC proteins from Rous sarcoma virus and human immunodeficiency virus type 1. *J. Virol.*, **69**, 6487–6497.

Campbell,S. and Vogt,V.M. (1997) *In vitro* assembly of virus-like particles with Rous sarcoma virus Gag deletion mutants: identification of the p10 domain as a morphological determinant in the formation of spherical particles. *J. Virol.*, **71**, 4425–4435.

Caspar,D.L.D. and Klug,A. (1962) Physical principles in the construction of regular viruses. *Cold Spring Harb. Symp. Quant. Biol.*, **27**, 1–24.

Coffin,J.M., Hughes,S.H. and Varmus,H.E. (1997) *Retroviruses*. Cold Spring Harbor Laboratory Press, Cold Spring Harbor, NY.

de Haas,F., Paatero,A.O., Mindich,L., Bamford,D.H. and Fuller,S.D. (1999) A symmetry mismatch at the site of RNA packaging by the polymerase complex of dsRNA bacteriophage phi-6. *J. Mol. Biol.*, **294**, 357–372.

Ehrlich,L.S., Agresta,B.E. and Carter,C.A. (1992) Assembly of recombinant human immunodeficiency virus type 1 capsid protein *in vitro*. *J. Virol.*, **66**, 4874–4883.

Erickson,H.P. and Klug,A. (1971) Measurement and compensation of defocusing and aberrations by Fourier processing of micrographs. *Phil. Trans. R. Soc. Lond. B*, **261**, 105–118.

Frank,J., Radermacher,M., Penczek,P., Zhu,J., Li,Y., Ladjadj,M. and Leith,A. (1996) SPIDER and WEB: Processing and visualization of images in 3D electron microscopy and related fields. *J. Struct. Biol.*, **116**, 190–199.

Freed,E.O. (1998) HIV-1 Gag protein: Diverse functions in the virus life cycle. *Virology*, **251**, 1–15.

Fuller,S.D., Wilk,T., Gowen,B.E., Krausslich,H.G. and Vogt,V.M. (1997) Cryo-electron microscopy reveals ordered domains in the immature HIV-1 particle. *Curr. Biol.*, **7**, 729–738.

Gamble,T.R., Yoo,S., Vajdos,F.F., von Schwedler,U.K., Worthylake,D.K., Wang,H., McCutcheon,J.P., Sundquist,W.I. and Hill,C.P. (1997) Structure of the carboxyl-terminal dimerization domain of the HIV-1 capsid protein. *Science*, **278**, 849–853.

Ganser,B.K., Li,S., Klishko,V.Y., Finch,J.T. and Sundquist,W.I. (1999) Assembly and analysis of conical models for the HIV-1 core. *Science*, **283**, 80–83.

Ge,M. and Sattler,K. (1994) Observation of fullerene cones. *Chem. Phys. Lett.*, **220**, 192–196.

Gelderblom,H.R. (1991) Assembly and morphology of HIV: potential effect of structure on viral function. *AIDS*, **5**, 617–638.

Gelderblom,H.R., Hausmann,E.H.S., Örzel,M., Pauli,G. and Koch,M.A. (1987) Fine structure of human immunodeficiency virus (HIV) and immunolocalization of structural proteins. *Virology*, **156**, 171–176.

Goettlinger,H. (2001) The HIV-1 assembly machine. *AIDS*, **15**, S13–S20.

Grief,C., Nermut,M.V. and Hockley,D.J. (1994) A morphological and immunolabelling study of freeze-substituted human and simian immunodeficiency viruses. *Micron*, **25**, 119–128.

Gross,I., Hohenberg,H., and Krausslich (1997) *In vitro* assembly properties of purified bacterially expressed capsid proteins of human immunodeficiency virus. *Eur. J. Biochem.*, **249**, 592–600.

Gross,I., Hohenberg,H., Wilk,T., Wiegers,K., Grättinger,M., Muller,B., Fuller,S. and Kräusslich,H.G. (2000) A conformational switch controlling HIV-1 morphogenesis. *EMBO J.*, **19**, 103–113.

Kakker,N.K., Mikhailov,M.V., Nermut,M.V., Burny,A. and Roy,P. (1999) Bovine leukemia virus Gag particle assembly in insect cells: formation of chimeric particles by domain-switched leukemia/lentivirus Gag polyprotein. *Virology*, **265**, 308–318.

Kingston,R.L., Olson,N.H. and Vogt.V.M. (2001) The organization of mature Rous sarcoma virus as studied by cryo-electron microscopy. *J. Struct. Biol.*, **136**, 67–80.

Kotov,A., Zhou,J., Flicker,P. and Aiken,C. (1999) Association of Nef with the human immunodeficiency virus type 1 core. *J. Virol.*, **73**, 8824–8830.

Li,S., Hill,C.P., Sundquist,W.I. and Finch,J.T. (2000) Image reconstructions of helical assemblies of the HIV-1 CA protein. *Nature*, **407**, 409–413.

Mancini,E.J., Clarke,M., Gowen,B., Rutten,T. and Fuller,S.D. (2000) Cryo-electron microscopy reveals the functional anatomy of an enveloped virus, Semliki Forest virus. *Mol. Cell*, **5**, 255–266.

Mancini,E.J. and Fuller,S.D. (2000) Supplanting crystallography or supplementing microscopy? A combined approach to the study of an enveloped virus. *Acta Crystallogr. D*, **56**, 1278–1287.

Mayo,K., McDermott,J. and Barklis,E. (2002a) Hexagonal organization of Moloney murine leukemia virus capsid proteins. *Virology*, **298**, 30–38.

Mayo,K., Vana,M.L., McDermott,J., Huseby,D., Leis,J. and Barklis,E. (2002b) Analysis of Rous sarcoma virus capsid protein variants assembled on lipid monolayers. *J. Mol. Biol.*, **316**, 667–678.

McDermott,J., Mayo,K. and Barklis,E. (2000) Three-dimensional organization of retroviral capsid proteins on a lipid monolayer. *J. Mol. Biol.*, **302**, 121–133.

Nermut,M.V., Hockley,D.J., Jowett,J.B., Jones,I.M., Garreau,M. and Thomas,D. (1994) Fullerene-like organization of HIV gag-protein shell in virus-like particles produced by recombinant baculovirus. *Virology*, **198**, 288–296.

Nermut,M.V., Bron,P., Thomas,D., Rumlova,M., Ruml,T. and Hunter,E. (2002) Molecular organization of Mason–Pfizer monkey virus capsids assembled from Gag polyprotein in *Escherichia coli*. *J. Virol.*, **76**, 4321–4330.

Parker,S.D., Wall,J.S. and Hunter,E. (2001) Analysis of Mason–Pfizer monkey virus Gag particles by scanning transmission electron microscopy. *J. Virol.*, **75**, 9543–9548.

Scarlata,S., Ehrlich,L.S. and Carter,C.A. (1998) Membrane-induced alterations in HIV-1 Gag and matrix protein–protein interactions. *J. Mol. Biol.*, **277**, 161–169.

Sepkowitz,K.A. (2001) AIDS—the first 20 years. *N. Engl. J. Med.*, **344**, 1764–1772.

Vogt,V.M. (1997) Retroviral virions and genomes. In Coffin,J.M., Hughes,S.H. and Varmus,H.E. (eds), *Retroviruses*. Cold Spring Harbor Laboratory Press, Cold Spring Harbor, NY, pp. 27–70.

Welker,R., Hohenberg,H., Tessmer,U., Huckhagel,C. and Krausslich,H.G. (2000) Biochemical and structural analysis of isolated mature cores of human immunodeficiency virus type 1. *J. Virol.*, **74**, 1168–1177.

Wilk,T., Gowen,B.E. and Fuller,S.D. (1999) Actin associates with the nucleocapsid domain of the Gag polyprotein in the human immunodeficiency virus (HIV-1). *J. Virol.*, **73**, 1931–1940.

Wilk,T., Gross,I., Gowen,B.E., Rutten,T., de Haas,F., Welker,R., Krausslich,H.G., Boulanger,P. and Fuller,S.D. (2001) Organization of immature human immunodeficiency virus type 1. *J. Virol.*, **75**, 759–771.

Worthylake,D.K., Wang,H., Yoo,S., Sundquist,W.I. and Hill,C.P. (1999) Structures of the HIV-1 capsid protein dimerization domain at 2.6 Å resolution. *Acta Crystallogr. D*, **55**, 85–92.

Yacobsen,B.I. and Smalley,R.E. (1997) Fuller nanotubes: $C1,0_0 0,0_{00}$ and beyond. *Am. Scientist*, **85**, 324–337.

Yeager,M., Wilson-Kubalek,E.M., Weiner,S.G., Brown,P.O. and Rein,A. (1998) Supramolecular design of native and immature murine leukemia virus revealed by electron cryo-microscopy. *Proc. Natl Acad. Sci. USA*, **95**, 7299–7304.

Yu,F., Joshi,S.M., Ma,Y.M., Kingston,R.L., Simon,M.N. and Vogt,V.M. (2001) Characterization of Rous sarcoma virus Gag particles assembled *in vitro*. *J. Virol.*, **75**, 2753–2764.

Received September 30, 2002; revised February 3, 2003; accepted February 4, 2003